

Contents lists available at ScienceDirect

#### Behavioural Brain Research

journal homepage: www.elsevier.com/locate/bbr



#### Research article

## Fear learning sculpts functional brain connectivity at rest beyond the traditional fear network

Christoph Fraenz<sup>a,\*</sup>, Dorothea Metzen<sup>b</sup>, Christian J. Merz<sup>c</sup>, Helene Selpien<sup>d</sup>, Patrick Friedrich<sup>e</sup>, Sebastian Ocklenburg<sup>f,g,h</sup>, Nikolai Axmacher<sup>i</sup>, Erhan Genç<sup>a</sup>

- a Department of Psychology and Neurosciences, Leibniz Research Centre for Working Environment and Human Factors (IfADo), Dortmund 44139, Germany
- <sup>b</sup> Department of Clinical and Biopsychology, Institute of Psychology, Faculty of Educational Sciences and Psychology, TU Dortmund University, Dortmund 44227, Germany
- <sup>c</sup> Department of Cognitive Psychology, Institute of Cognitive Neuroscience, Faculty of Psychology, Ruhr University Bochum, Bochum 44801, Germany
- <sup>d</sup> Klinik für Anästhesiologie und Operative Intensivmedizin, Universitätsklinikum Schleswig-Holstein, Kiel 24105, Germany
- <sup>e</sup> Department "Brain and Behaviour", Institute of Neuroscience and Medicine, Forschungszentrum Jülich, Jülich 52428, Germany
- f Department of Psychology, Faculty of Human Sciences, Medical School Hamburg, Hamburg 20457, Germany
- g ICAN Institute for Cognitive and Affective Neuroscience, Medical School Hamburg, Hamburg 20457, Germany
- h Department of Biopsychology, Institute of Cognitive Neuroscience, Faculty of Psychology, Ruhr University Bochum, Bochum 44801, Germany
- Department of Neuropsychology, Institute of Cognitive Neuroscience, Faculty of Psychology, Ruhr University Bochum, Bochum 44801, Germany

#### ARTICLE INFO

# Keywords: Fear acquisition Fear consolidation Resting-state Functional brain connectivity Functional magnetic resonance imaging Fear network Safety network

#### ABSTRACT

Neuroscientific research has identified specific brain networks involved in the acquisition of fear memories. Using functional magnetic resonance imaging to assess changes in resting-state functional connectivity (RSFC) induced by fear acquisition, single brain regions from these networks have been linked to fear memory consolidation. However, previous studies merely examined RSFC changes within restricted sets of brain regions or without a proper control group, leaving our knowledge about fear consolidation outside of traditional fear networks incomplete. Here, an experimental group of 98 and a control group of 28 individuals, free of selfreported psychiatric or neurological disorders, participated in a differential fear conditioning paradigm using visual stimuli and electrical stimulation. Fear responses were quantified by skin conductance responses. RSFC changes were analyzed across 360 cortical and 16 subcortical brain regions, constituting a total of 70,500 functional connections. Subsequent to fear acquisition, we identified 21 functional connections, involving 35 individual brain regions, that exhibited significant RSFC changes in the experimental compared to the control group. Importantly, these connections were not restricted to traditional fear networks but also comprised various frontal, visual, premotor, and somatosensory regions. Overall, our findings highlight the importance of employing a proper control group and indicate that fear memory consolidation is a complex process that integrates relevant information across the entire brain. Brain regions recruited for this task presumably depend on the modality of acquired fear memories, which demands an update regarding the components of established fear networks.

#### 1. Introduction

The acquisition, maintenance, and extinction of conditioned fear responses are critical functions that help us to evaluate and differentiate potential threats and safety signals in the environment [12,60]. Understanding the neural mechanisms tied to these fear learning processes is essential not only for advancing our fundamental knowledge of brain

function but also for developing targeted neural interventions that could benefit patients suffering from anxiety disorders. However, our understanding of how fear learning affects the brain's functional connectome remains limited.

In order to study fear learning under experimental conditions, most studies employ classical Pavlovian fear conditioning paradigms. Usually, these experiments involve the repetitive presentation of two neutral

E-mail address: fraenz@ifado.de (C. Fraenz).

<sup>\*</sup> Corresponding author at: Department of Psychology and Neurosciences, Leibniz Research Centre for Working Environment and Human Factors (IfADo), Ardeystraße, Dortmund 44139, Germany.

stimuli (e.g., tones or pictures) of which one is always or partially reinforced with an aversive stimulus (e.g., an unpleasant electric shock), also known as the unconditioned stimulus (US). As a consequence, the former neutral stimuli become conditioned stimuli (CS) and subjects typically show a conditioned fear response (CR) towards the reinforced stimulus (CS+) but not the non-reinforced stimulus (CS-). The degree of CR can be assessed by means of skin conductance responses (SCRs) or fear ratings for example [50].

The combination of fear acquisition training and neuroimaging methods such as functional magnetic resonance imaging (fMRI) provides an opportunity to reveal specific brain areas involved in fear learning. In humans, respective efforts were able to identify a brain network comprising hippocampus, amygdala, dorsal anterior cingulate cortex, ventromedial prefrontal cortex, and insula [58]. This so-called "fear network" could later be refined by a large-scale meta-analysis of fMRI studies on fear learning in humans which identified not one but two complementary brain networks [23]. The first network is constituted by brain regions that are primarily active during CS+ presentation, which suggests a strong involvement in the processing of potential threat. The respective network strongly resembles what has previously been described as the fear network. In contrast, brain regions from the second network are highly active in response to CS- presentation. Given its vital role in processing non-threatening stimuli, the respective network has been coined the "safety network" [23]. It comprises the hippocampus, ventromedial prefrontal cortex, lateral orbitofrontal cortex, and posterior cingulate cortex.

Although fear memories are rapidly acquired [67], subsequent offline processing known as memory consolidation, is required for shaping and maintaining a rich and diverse array of fear-related behaviors. One way to examine fear memory consolidation in humans is to assess brain activity while the brain is "at rest". Again, this can be achieved by neuroimaging methods such as fMRI, which are able to quantify resting-state functional connectivity (RSFC) before and after fear learning. RSFC is typically defined as the mutual low-frequency fluctuations in activity that occur across two or more brain regions during the absence of sensory input [21]. However, intrinsic brain activity during periods of rest may not be devoted exclusively to default-mode processing. Alternative perspectives propose that the resting brain actively and selectively processes previous experiences [57]. Measures of RSFC are relatively stable across time [10]. However, changes in functional connectivity following behavioral tasks have been observed, especially during immediate post-encoding time periods in which initial stages of memory consolidation are likely to unfold [34]. In addition, RSFC patterns observed shortly after a specific task resemble the expression of functional connectivity during that task. Such effects have been reported for motor learning [1,86], visual perceptual learning [30,45], attention [11], as well as working memory [28], and lexico-semantic cognition [74].

It has been demonstrated that fear learning processes can alter the RSFC between specific brain regions from the fear and safety networks. These include the amygdala, dorsal anterior cingulate cortex, ventromedial prefrontal cortex, insula, and hippocampus [16,17,34,76,87]. However, respective studies entail certain methodological and conceptual limitations, which require further investigation. First, some studies did not assess RSFC changes in a control group, restricting their analyses to a single within-group comparison [34,76,87]. Thus, it cannot be ruled out that reported RSFC changes were caused by factors other than fear learning. Second, while most studies conducted functional connectivity analyses that involved regions from the entire brain, they also employed pre-defined seed regions such as the amygdala [16,76,87]. This approach neglects all functional connections that are not part of the network studied under these a priori assumptions, for example, any interplay between visual and cingular regions. Due to this lack of unrestricted whole-brain analyses, it currently remains underexplored whether fear learning induces RSFC changes outside of the fear and safety networks. Considering that fear learning often takes place in

situations that also involve a variety of cognitive, emotional, and social processes, it is plausible that the fear and safety networks need to interact closely with other brain networks supporting these functions.

In summary, it has been shown that the differentiation between threatening and non-threatening stimuli is primarily associated with activation patterns in two neural networks known as the fear network and safety networks. Changes in RSFC can be used as a measure to study consolidation processes after fear acquisition. Despite the complexity of fear learning, previous fMRI studies from this line of research widely neglected functional connections outside of the fear and safety networks. To address this issue, the study at hand aimed to follow a data driven and explorative approach without making any a priori assumptions regarding the connections or networks to study. Consequentially, we examined RSFC changes within the whole brain and investigated RSFC changes between 360 cortical and 16 subcortical brain areas occurring subsequent to fear acquisition training. We conducted three analyses that involved a within-group comparison, a correlation analysis that aimed to associate RSFC changes with the magnitude of CR as quantified by SCRs, and a between-group comparison. By doing so, we observed expected RSFC changes in functional connections from the fear and the safety network. Interestingly, we were also able to identify RSFC changes in functional connections involving brain regions not included in the traditional fear and safety networks. Among these were visual, frontal, premotor, and somatosensory regions, suggesting a complex integration of information that was likely shaped by the modalities targeted in our fear acquisition paradigm.

#### 2. Materials and methods

#### 2.1. Participants

For this study, we recruited 165 participants, free of self-reported psychiatric or neurological disorders. They were randomly assigned to an experimental group (N = 137), which underwent a fear acquisition paradigm with electrical stimulation (see 2.2. Fear Acquisition Paradigm), and a control group (N = 28), to which the same stimuli were presented but without electrical stimulation. This was done to examine potential effects of fear acquisition by means of between-group analysis (see 2.7. Statistical Analysis). In total, 39 participants from the experimental group had to be excluded due to various reasons. Twenty-seven participants were classified as "non-responders" since they did not show valid SCRs in reaction to any of the US presentations (at least 0.05  $\mu$ S) [49]. Twelve participants reported a CS-/US contingency that was equal to or larger than the reported CS+ /US contingency, indicating absent contingency awareness [85]. Hence, all imaging analyses were carried out with data from the remaining 126 participants (76 women).

The final sample, comprising the experimental as well as the control group, had an age range from 18 to 26 years (M = 21.81, SD = 2.12). We did not observe significant age differences between male and female participants (t(124) = 1.426, p = .157). The experimental group included 98 participants (55 women) with a mean age of 21.94 years (SD = 2.00) and the control group included 28 participants (21 women) with a mean age of 21.36 years (SD = 2.48). Both groups did not differ significantly with regard to age (t(124) = 1.284, p = .202) or sex (X²(1, N = 126) = 3.242, p = .072). We also did not observe statistically significant age differences between male and female participants within the experimental (t(96) = 1.187, p = .238) or the control group (t (26) = 0.433, p = .669).

The final sample was also rather homogenous with respect to race and ethnicity. Since genetic data were collected for analyses unrelated to the study at hand, it had to be ensured that the vast majority of participants was of European descent. To this end, participants were asked about the birthplace of their grandparents during screening. On average, participants reported that three out of their four grandparents were born in Germany. This ratio did not differ between the experimental (73.6 %) and the control (75.9 %) group.

In addition to genetic data, psychometric data on trait anxiety and information processing capacity were also collected as part of a different project. Trait anxiety was measured via the State-Trait Anxiety Inventory [43] and did not differ between the experimental (M=37.4) and control (M=38.4) group (t(119)=-0.637, p=0.525). Information processing capacity was captured via the Zahlen-Verbindungs-Test [64], a test of perceptual speed similar to the Trail Making Test. Again, results did not show significant differences between the experimental (M=56.3 s) and control (M=56.2 s) group (t(121))=0.017, p=0.987).

In order to control for any potential effects caused by handedness, only right-handed individuals were recruited, as measured by the Edinburgh Handedness Inventory [63]. All participants had normal or corrected-to-normal vision and were able to understand the instructions given to them orally or in writing. They were either paid for their participation or received course credit. All participants were naive to the purpose of the study and had no former experience with the aversive learning paradigm used for the experiment. Participants reported no history of psychiatric or neurological disorders and matched the standard inclusion criteria for fMRI examinations. The study was approved by the local ethics committee of the Faculty of Psychology at Ruhr University Bochum. All participants provided written informed consent prior to participation and were treated in accordance with the Declaration of Helsinki.

#### 2.2. Fear acquisition paradigm

While in the MRI scanner, all participants completed differential fear acquisition training followed by fear extinction training. Importantly, only participants from the experimental group received electrical stimulation during fear acquisition. In contrast, participants from the control group received no electrical stimulation. Beyond that, participants from both groups underwent the same experimental procedures. Resting-state measurements of around 8 min were conducted prior to fear acquisition training, in between both phases, and after fear extinction training. As this study is only concerned with fear acquisition training, all procedures related to fear extinction training will be reported elsewhere. The stimuli and procedure used for fear acquisition training were modified from Milad et al. [59].

After arrival, participants gave written informed consent and filled out a questionnaire on demographic variables. Prior to scanning, all participants were instructed to close their eyes during resting-state scans and to pay close attention to the images being presented during fear acquisition training. They were also told that electrical stimulation may or may not be presented during the experiment. The experimental group and the control group received identical instructions. The electrical stimulation (1 ms pulses with 50 Hz for a duration of 100 ms) was applied as the US using a constant voltage stimulator (STM2000, BIO-PAC Systems, Goleta, CA, USA) along with two electrodes attached to the fingertips of the first and second fingers of the right hand. The intensity of the electrical stimulation was adjusted for each participant individually prior to the first resting-state scan. For this purpose, electrical stimulation was administered at 30 V and raised in increments of 5 V until participants rated the sensation as very unpleasant but not painful.

During fear acquisition training, participants were shown pictures of an office room with a switched off desk lamp (Fig. 1, top). In each trial, the desk lamp would either light up in blue (CS+) or in yellow (CS-), which served as the two CS. The images were presented using the Presentation software package (Neurobehavioral Systems, Berkeley, CA, USA) and MR suitable LCD-goggles (Visuastim Digital, Resonance Technology, Northridge, CA, USA). At the beginning of each trial, a white fixation cross was presented on a black background for 6.8–9.5 s. Next, the office room image was presented for 1 s, which was followed by the presentation of the CS+ or the CS- for another 6 s. In the experimental group, the CS+ was paired with the electrical stimulation in 62.5 % of trials (10 out of 16 trials). The stimulation was administered

5.9 s after CS+ onset and co-terminated with CS+ offset. Across all 32 trials, CS+ and CS- were presented 16 times each in pseudo-randomized order. The first two trials always consisted of one CS+ and one CS-presentation and so did the last two trials. In the experimental group, the first and last CS+ presentations were always paired with the electrical stimulation. There were no trials that presented the same type of CS more than twice in consecutive order. CS+ and CS- presentations were distributed equally across both halves of fear acquisition.

After fear acquisition training, participants had to rate the contingencies between CS+ , CS-, and US. First, they were asked to report the number of electrical stimulations they had received during the experiment. In addition, participants from the experimental group were asked to rate the unpleasantness of the last electrical stimulation on a 9-point Likert scale (1 - "not unpleasant", 9 - "very unpleasant") and to report at what rate the blue lamplight and the yellow lamplight had been followed by an electrical stimulation. In contrast, participants from the control group were asked if they had noticed any differences between the two images and how often the blue and the yellow lamplights were presented.

#### 2.3. Acquisition of imaging data

All imaging data were acquired at the Bergmannsheil hospital in Bochum, Germany, using a 3 T Philips Achieva scanner with a 32-channel head coil. Scanning included anatomical imaging, task-based imaging, and resting-state imaging.

#### 2.3.1. Anatomical imaging

For the purpose of coregistration and brain parcellation, both necessary steps in the connectivity analyses performed in this study, T1-weighted high-resolution anatomical images were acquired (MP-RAGE, TR = 8.2 ms, TE = 3.7 ms, flip angle =  $8^{\circ}$ , 220 slices, matrix size = 240 mm×240 mm, resolution = 1 mm×1 mm x 1 mm). Scanning time was around 6 min.

#### 2.3.2. Task-based imaging

In order to identify specific brain regions showing a significantly pronounced or diminished BOLD response during fear acquisition training, we employed echo planar imaging. We obtained a time series of fMRI volumes for each participant from the experimental group while completing fear acquisition training (TR =2500 ms, TE =35 ms, flip angle  $=90^{\circ}$ , 40 slices, matrix size =112 mm  $\times$  112 mm, resolution =2 mm  $\times$  2 mm  $\times$  3 mm). The same scanning protocol was used in the control group but obtained imaging data were not used for further analysis. In both cases, scanning time was around 8 min.

#### 2.3.3. Resting-state imaging

For the analysis of functional brain connectivity, fMRI resting-state images were acquired before and after fear acquisition training using echo planar imaging (TR = 2500 ms, TE = 30 ms, flip angle = 90°, 40 slices, matrix size = 112 mm $\times112$  mm, resolution = 2 mm $\times2$  mm x 3 mm). Scanning time of each resting-state scan was around 8 min.

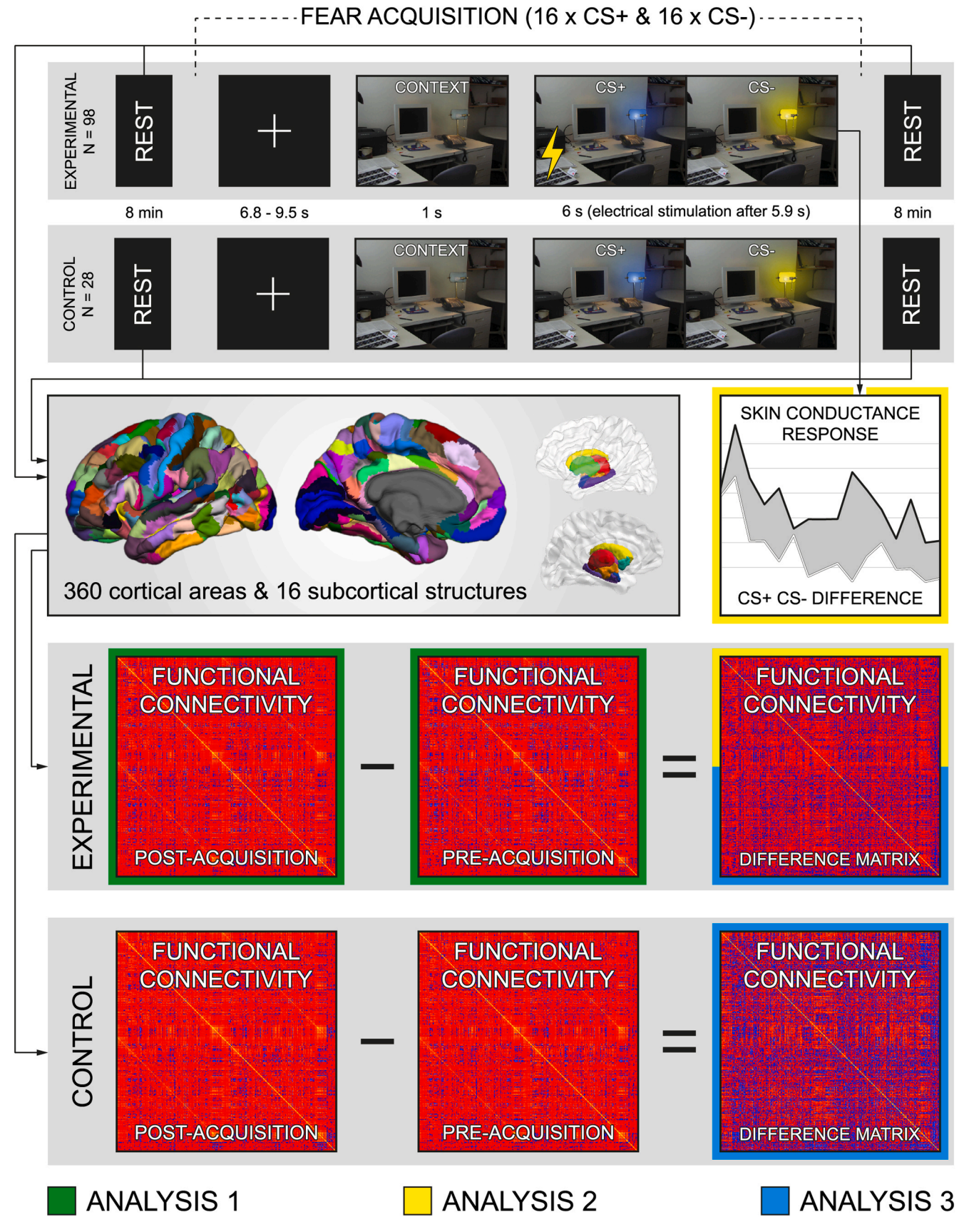
#### 2.4. Acquisition of skin conductance responses

Skin conductance responses were assessed using two Ag/AgCl electrodes filled with isotonic (0.05 NaCl) electrolyte medium placed on the hypothenar eminence right below the fifth finger of the left hand. Data were recorded using Brain Vision Recorder software (Brain Products, Munich, Germany).

#### 2.5. Analysis of imaging data

#### 2.5.1. Analysis of anatomical data

For the purpose of reconstructing the cortical surfaces of T1-weighted images, we used published surface-based methods in



(caption on next page)

Fig. 1. Data acquisition and analysis. The overall sample was split into an experimental (N = 98) and a control group (N = 28). While in the scanner, both groups participated in fear acquisition training that was preceded and followed by 8-minute-long fMRI resting-state scans. At the beginning of each trial, a white fixation cross was presented on a black background for 6.8–9.5 s. Next, the image of an office room was presented for 1 s, which was followed by the presentation of the CS+ (blue lamplight) or the CS- (yellow lamplight) for another 6 s. In the experimental group, the CS+ was paired with electrical stimulation as the US (indicated by a yellow bolt) in 62.5 % of trials administered 5.9 s after CS+ onset. The CS+ and CS- were presented 16 times each in pseudo-randomized order. In both groups, brain images obtained from fMRI resting-state scans were parcellated into 360 cortical areas and 16 subcortical structures. The resulting ROIs were subjected to a functional connectivity analysis using BOLD signal correlations. For both groups separately, functional connectivity values from the pre-acquisition matrix in order to obtain a difference matrix. In the experimental group, fear learning was quantified by subtracting average skin conductance responses of CS- trials from those of CS+ trials. For the first analysis, indicated by green frames, the pre-acquisition matrices of the experimental group were compared. Functional connections exhibiting statistically significant differences were subjected to two additional analyses. For the second analysis, indicated by yellow frames, the conditioned fear response, as quantified via skin conductance responses, was correlated with functional connectivity values from the difference matrix of the experimental group. Functional connectivity values from the pre-acquisition matrix were used as a control variable. For the third analysis, indicated by light blue frames, the difference matrix of the experimental group was compared to that of the control group. Finally,

FreeSurfer (version 6.0.0, <a href="http://surfer.nmr.mgh.harvard.edu">http://surfer.nmr.mgh.harvard.edu</a>) along with the CBRAIN platform [80]. The details of this procedure have been described elsewhere [13,19]. The automatic reconstruction steps included skull stripping, gray and white matter segmentation as well as reconstruction and inflation of the cortical surface. These pre-processing steps were performed for each participant individually. Subsequently, each individual segmentation was quality-controlled slice by slice and inaccuracies of the automatic steps were corrected by manual editing if necessary.

Functional connectivity changes in resting-state data were analyzed between areas defined by the Human Connectome Project's multi-modal parcellation (HCPMMP) [27] as well as FreeSurfer's automatic subcortical segmentation (Fig. 1, middle). The HCPMMP delineates 180 cortical brain regions per hemisphere and is based on the cortical architecture, function, connectivity, and topography from 210 healthy individuals. From FreeSurfer's automatic subcortical segmentation, we included a set of eight subcortical structures per hemisphere (thalamus, caudate nucleus, putamen, pallidum, hippocampus, amygdala, accumbens area), various ventricle masks (lateral ventricle, inferior lateral ventricle, third ventricle, fourth ventricle), and a mask covering the whole cerebral white matter compartment [18]. In total, 360 cortical masks, 16 subcortical masks, 8 ventricle masks, and one white matter mask were linearly transformed into the native spaces of the resting-state images that were obtained before and after fear acquisition training. The respective masks served as regions of interest (ROIs) that were used for the functional connectivity analyses.

#### 2.5.2. Analysis of task-based data

Task-based data were analyzed by means of FEAT, which is part of the FSL toolbox (version 6.0.1, http://www.fmrib.ox.ac.uk/fsl). Preprocessing of respective images involved motion- and slice-timing correction, spatial smoothing with a 6 mm FWHM Gaussian kernel, high-pass filtering with the cutoff set to 50 s, linear registration to the individual's high-resolution T1-weighted anatomical image, and nonlinear registration to the standard stereotaxic space template of the Montreal Neurological Institute. First-level analyses employed a general linear model in order to generate two statistical maps of functional activation (CS+ > CS- and CS- > CS+) including data from all 16 CS+ and 16 CS- presentations. All six regressors (office image before CS presentation, CS+, CS-, US, US omission after CS+ presentation, non-US after CS- presentation) were modeled based on a stick function that was convolved with the canonical hemodynamic response function, without specifically modeling the durations of the different events (i.e., eventrelated design). Second-level analyses employed random-effects estimation by means of FLAME (FMRIB's Local Analysis of Mixed Effects). We utilized an FWE-corrected cluster thresholding option, p-values < .05, and Z-values > 3.1.

#### 2.5.3. Analysis of resting-state data

Resting-state data were pre-processed using MELODIC, which is also part of the FSL toolbox. Images were pre-processed in a number of steps:

Discarding the first two EPI volumes from each resting-state scan to allow for signal equilibration, motion and slice-timing correction, and high-pass temporal frequency filtering (0.005 Hz). Spatial smoothing was not applied in order to avoid the introduction of spurious correlations in neighboring voxels. For each ROI, we calculated a mean resting-state time course by averaging the pre-processed time courses of corresponding voxels.

We computed partial correlations between the average time courses of all 360 cortical and 16 subcortical regions, while controlling for several nuisance variables. We regressed out the trajectories of 6 head motion parameters as well as the mean time courses extracted from the white matter and ventricle masks [25]. The resulting correlation coefficients were subjected to a Fisher z-transformation [20] in order to receive normally distributed data suitable for further testing. By following this approach, we obtained two symmetrical 376-by-376 matrices with data assessed before (Supplementary Figure 1 and Supplementary Figure 2) and after fear acquisition training (Supplementary Figure 3 and Supplementary Figure 4), respectively (Fig. 1, bottom). Each cell of the two matrices contained a Fisher transformed correlation coefficient as a measure of functional connectivity between a specific pair of ROIs. Accounting for the symmetry of both matrices as well as self-correlations on their diagonals, each matrix comprised 70,500 individual connections. For each participant we calculated the difference between both matrices by subtracting the pre-acquisition matrix from the post-acquisition matrix (Supplementary Figure 5 and Supplementary Figure 6).

#### 2.6. Analysis of skin conductance responses

Raw SCR data from the experimental group were pre-processed with Brain Vision Analyzer software (Brain Products, Munich, Germany). All further analyses were conducted semi-automatically using MATLAB (R2022b, The MathWorks, Natick, MA, USA). SCR to CS presentation was defined as the maximum amplitude recorded within the time window starting 1 s after CS onset and ending 6.5 s after CS onset. CR was defined as the difference between the average SCR across CS+ trials and the average SCR across CS- trials (Fig. 1, middle). Additionally, SCR to US presentation was defined as the maximum amplitude recorded within the time window starting 6.5 s after CS onset and ending 12 s after CS onset. The unconditioned response was quantified as the difference between the average SCR across CS+ trials with electrical stimulation and the average SCR across CS- trials.

#### 2.7. Statistical analysis

All statistical analyses were carried out using MATLAB (version R2022b, The MathWorks Inc., Natick, MA). For all analyses, we employed linear parametric methods. Testing was two-tailed with an  $\alpha$ -level of .05, which was corrected for multiple comparisons using the Benjamini-Hochberg method [8]. We conducted three statistical analyses, with the results of the first analysis informing the second and third

analyses.

First, we performed paired-sample t-tests between functional connectivity values from the pre-acquisition and the post-acquisition matrices. Here, our goal was to assess which of the 70,500 functional connections showed significant increases or decreases in their Fisher-transformed BOLD signal correlations after fear acquisition training. Hence, respective tests were carried out for the experimental group exclusively and corrected  $\alpha\text{-levels}$  were in the range between .05 / 70,500 = .0000007 and .05 as defined by the Benjamini-Hochberg method.

Second, all functional connections reaching statistical significance in the first analysis were considered for the second analysis. Here, our goal was to examine the association between aforementioned functional connectivity changes and the SCRs obtained during fear acquisition training. To this end, we computed partial correlations between the functional connectivity values from the experimental group's difference matrix (see 2.5.3. Analysis of Resting-state Data) and their conditioned fear responses. Functional connectivity values from the pre-acquisition matrix were used as a control variable. Recent studies have demonstrated that healthy individuals can exhibit fear generalization during fear acquisition training [83], i.e., by showing fear responses to both CS+ and CS- presentations. In such cases, differential responses (CS+ CS-) may not serve as an appropriate measure of fear learning. Therefore, we also carried out said partial correlation analysis with CS+ and CS- responses instead of differential responses.

Third, the same functional connections considered for the second analysis were subjected to a comparison between the experimental and control group. For this purpose, the experimental group's difference matrix was compared to that of the control group using two-sample t-tests. Again, we accounted for multiple comparisons by using the Benjamini-Hochberg method and adjusted the  $\alpha$ -levels according to the number of functional connections that exhibited statistical significance after the first analysis.

Given the large number of brain regions involved in the analyses, we decided to repeat the second and third analyses while following a leave-one-out cross-validation approach with stability selection. More specifically, 97 iterations of the second analysis (partial correlations in the experimental group) and 125 iterations of the third analysis (differences in RSFC changes between the experimental and control groups) were carried out. With each iteration, a different participant was excluded from the respective analysis. In the end, we identified functional connections that exhibited significant results across 90 % and 100 % of iterations, respectively. By ensuring that significant findings were robust across multiple subsamples, we enhanced the reliability of results, reduced the risk of false positives, and prevented overfitting.

In a final step, we checked the results yielded by the second and third analyses for overlaps. Only results generated by the same type of crossvalidation (no cross-validation, cross-validation with a 90 % replication threshold, cross-validation with a 100 % replication threshold) were matched against each other. The second, third, and overlap analyses in combination with the three types of cross-validation, resulted in nine different sets of connections. We used the connections from each set to extract the corresponding functional connectivity changes from participants' difference matrices. These values in turn served as data to implement a machine learning pipeline to classify each participant as belonging to either the experimental or the control group. The pipeline employed the Synthetic Minority Oversampling Technique (SMOTE) to address class imbalances in the training data, ensuring a balanced representation of the experimental and control group. Data scaling was applied to normalize the covariates, enabling the models to focus on patterns rather than raw magnitudes. To prevent overfitting, we used logistic regression models with elastic-net regularization (L1 + L2). Hyperparameters were tuned via grid search cross-validation. Each model's performance was evaluated using nested cross-validation, consisting of an outer 10-fold cross-validation loop to assess generalization to unseen data (approximately 113-114 subjects for training and 12–13 for testing per fold) and an inner 5-fold cross-validation loop to select optimal hyperparameters. We built nine models in total, one for each set of connections.

#### 3. Results

#### 3.1. Efficacy of fear acquisition training

Participants showed significantly greater SCRs in reaction to CS+ presentations relative to CS- presentations (t(97) = 6.525,p < .001) (Fig. 2), indicating successful fear learning. We also found a significant correlation between CRs and contingency ratings (r = 0.28, p < .001). This association indicates that the explicit knowledge participants had about shock occurrence was associated with the more implicit physiological level, namely in the mean difference between SCRs in reaction to CS+ and CS- presentations. Furthermore, fMRI data obtained during fear acquisition training revealed distinct patterns of functional activation in reaction to CS+ and CS- presentations. Overall, our data were in good accordance with the results of a large-scale metaanalysis on the functional correlates of fear acquisition [23]. Voxel clusters exhibiting significant (p < .01, Z > 2.3, FWE-corrected) BOLD signal contrasts in our data either overlapped with clusters from the fear and safety networks or were directly adjacent to them (Supplementary Figure 7 and Supplementary Figure 8). With regard to the fear network (contrast CS+ minus CS-), we were able to replicate core components like the anterior insular cortex, caudate nucleus, dorsal anterior cingulate cortex, and secondary somatosensory cortex. Likewise, core components from the safety network (contrast CS- minus CS+), namely the primary somatosensory cortex, dorsal anterior prefrontal cortex, parahippocampal gyrus, lateral orbitofrontal cortex, angular gyrus, and dorsal posterior precuneus, could also be identified.

#### 3.2. Functional connectivity changes in the experimental group

For our first analysis, we employed paired-sample t-tests to compare the experimental group's pre-acquisition matrices (Supplementary Figure 1) to its post-acquisition matrices (Supplementary Figure 3). In total, we observed 3089 functional connections (4.38 %) that exhibited

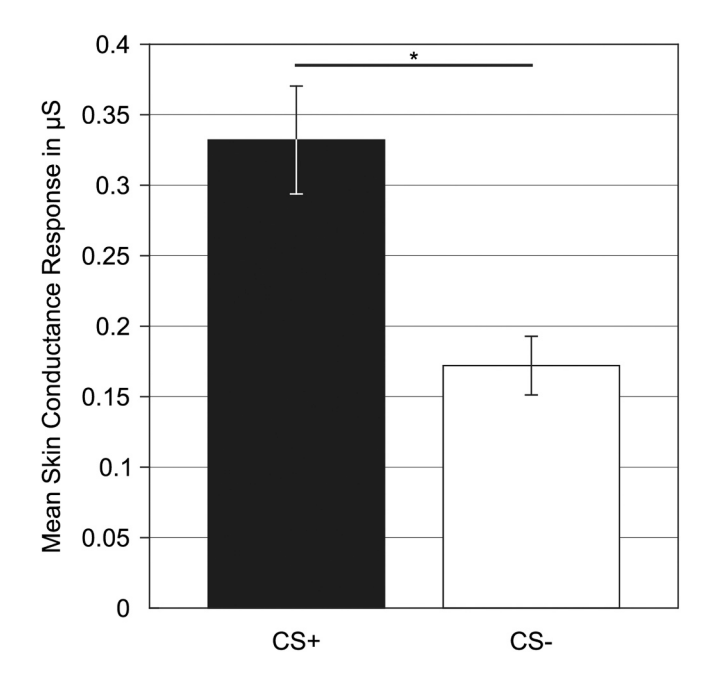


Fig. 2. Mean skin conductance responses. Bar plots showing the mean skin conductance responses in reaction to CS+ (black bar) and CS- (white bar) presentations in microSiemens ( $\mu$ S). Data were averaged across all 16 CS+ and 16 CS- trials, respectively. Error bars represent standard errors (\* p < .001).

significant changes after correction for multiple comparisons (Supplementary Table 1). It is noteworthy that 3059 out of these 3089 significant connections (99.03 %) showed increases in their Fisher-transformed BOLD signal correlations, meaning that positive coefficients became larger, negative coefficients became smaller, or negative coefficients became positive. This pronounced shift towards more positive coefficients was not only present among the 3089 significant connections but could also be observed for the overall functional connectome of the experimental group. Here, 53,409 out of 70,500 connections (75.76 %) showed increases, while only 17,091 (24.24 %) showed decreases. We observed a similar, albeit less pronounced ( $X^2(1, N = 141,000) = 2489.96$ , p < .001), pattern in the control group with 44,794 connections (63.54 %) showing increases and 25,706 connections (36.46 %) showing decreases.

## 3.3. Associations between functional connectivity changes and conditioned fear responses

Our second analysis involved all functional connections that exhibited statistically significant changes between the pre-acquisition and post-acquisition matrices (first analysis). We computed partial correlations between these RSFC changes and the participants' CR obtained via SCR during fear acquisition training (see 2.6. Analysis of Skin Conductance Responses). RSFC values from the pre-acquisition matrix were used as a control variable. As with the first analysis, the  $\alpha$ -levels were corrected using the Benjamini-Hochberg method and ranged from .05 / 3089 = .000016 to .05 given the number of functional connections (3089) that were considered. We identified 386 connections for which the correlations between RSFC changes and CR reached a level of  $\alpha$ = .05 (uncorrected). However, none of these correlations survived said correction for multiple comparisons (Supplementary Table 2). Among these 386 connections, 371 were positive (96.11 %) and 15 (3.89 %) were negative. The largest positive correlation was r=.4065 and the smallest was r=.2000. The largest negative correlation was r=-.3095and the smallest was r = -.2055. Almost all 386 significant connections (99.22 %) were constituted by two cortical areas and only three connections (0.78 %) involved one cortical and one subcortical area. We observed slightly more interhemispheric (54.92 %) than intrahemispheric (45.08 %) connections. In addition to partial correlations between RSFC changes and CR, we also computed partial correlations between RSFC changes and CS+ responses (Supplementary Table 3) as well as RSFC changes and CS- responses (Supplementary Table 4).

The second analysis was repeated while following a leave-one-out cross-validation approach with stability selection. Given that none of the correlations from the initial analysis survived a correction for multiple comparisons, we considered all results reaching a level of  $\alpha=.05$  (uncorrected) instead. Among the 386 connections yielded by the initial analysis, we identified 319 connections which replicated across 90 % of iterations and 173 which replicated across 100 % of iterations. The exact percentage value for each connection is provided in Supplementary Table 2.

#### 3.4. Group differences in functional connectivity changes

For our third analysis, we subjected all statistically significant connections from the first analysis to a comparison between the experimental and control group. For this purpose, we compared the difference matrices of the two groups (Supplementary Figure 5 and Supplementary Figure 6) with each other using two-sample t-tests. The  $\alpha$ -levels were corrected via the Benjamini-Hochberg method and covered the same range as in the second analysis. Again, there were no results that survived this correction. However, we identified 285 functional connections for which the t-test comparisons between experimental and control group RSFC changes reached a level of  $\alpha=.05$  (uncorrected) (Supplementary Table 5). The majority of these functional connections showed an increase of RSFC in the experimental group combined with a

decrease (80.00 %) or increase (16.84 %) of RSFC in the control group. Only 9 connections (3.16 %) showed a decrease in the experimental and an increase in the control group. We did not observe any connections exhibiting a decrease of RSFC in both the experimental and the control group. The 285 significant connections were either constituted by two cortical areas (92.98 %) or one cortical and one subcortical area (7.02 %). There were no connections running between two subcortical areas. We found a balanced distribution of intra- (50.18 %) and interhemispheric (49.82 %) connections. Changes in RSFC ranged from -0.0636 to 0.1321 in the experimental group and from -0.0845 to 0.2118 in the control group. The smallest group difference in RSFC changes still reaching a level of  $\alpha=.05$  (uncorrected) was 0.0524 and the largest such difference was 0.1358.

In an analogues manner to the second analysis, the third analysis was also repeated while following a leave-one-out cross-validation approach with stability selection. Again, we considered those results reaching a level of  $\alpha=.05$  (uncorrected). Among the 285 connections yielded by the initial analysis, we identified 251 connections which replicated across 90 % of iterations and 148 which replicated across 100 % of iterations. The exact percentage value for each connection is provided in Supplementary Table 5.

#### 3.5. Overlaps in results

Finally, we checked the results from the second and third analysis for overlaps. Since both analyses did not yield any significant results that survived the applied Benjamini-Hochberg correction for multiple comparisons, we examined all results reaching a level of  $\alpha = .05$  (uncorrected), namely 386 connections from the second and 285 connections from the third analysis. Among these, we found 21 matching connections (Fig. 3 and Table 1). All of these connections were constituted by two cortical areas. There were 12 interhemispheric connections and 9 intrahemispheric connections of which 5 were located in the left hemisphere and 4 were located in the right hemisphere. We also checked the results obtained from the alternate versions of the second analysis for potential overlaps with the results from the third analysis. Partial correlations between RSFC changes and CS+ responses yielded 28 matching connections (Supplementary Table 6) while partial correlations between RSFC changes and CS- responses yielded 21 matching connections (Supplementary Table 7).

The leave-one-out cross validation approach with stability selection identified the most robust results from the second and third analyses and yielded a smaller set of connections. A replication threshold of 90 % resulted in 319 connections for the second and 251 connections for the third analysis, among which we found 15 matching connections. An even stricter replication threshold of 100 % resulted in 173 connections for the second and 148 connections for the third analysis, among which we found only 3 matching connections. These different sets of connections are color-coded in Fig. 3 and highlighted in Table 1.

## 3.6. Accuracy of group classification derived from functional connectivity changes

To classify participants as belonging to either the experimental or the control group, we implemented a machine learning pipeline that used the functional connectivity changes corresponding to specific connections from nine different sets as features. We built and tested a model for each of these nine sets. The best performance across folds was achieved by models for which feature selection was derived from the results of the third analysis (differences in RSFC changes between the experimental and control groups). More specifically, cross-validation with a 90 % replication threshold performed best (251 features, 89.56  $\pm$  7.67 %), followed by cross-validation with a 100 % replication threshold (148 features, 87.39  $\pm$  8.37 %), and no cross-validation (285 features, 86.72  $\pm$  10.50 %). Feature selection derived from the results of the overlap analysis performed worse (3–21 features, 61.78–78.06 %) and feature

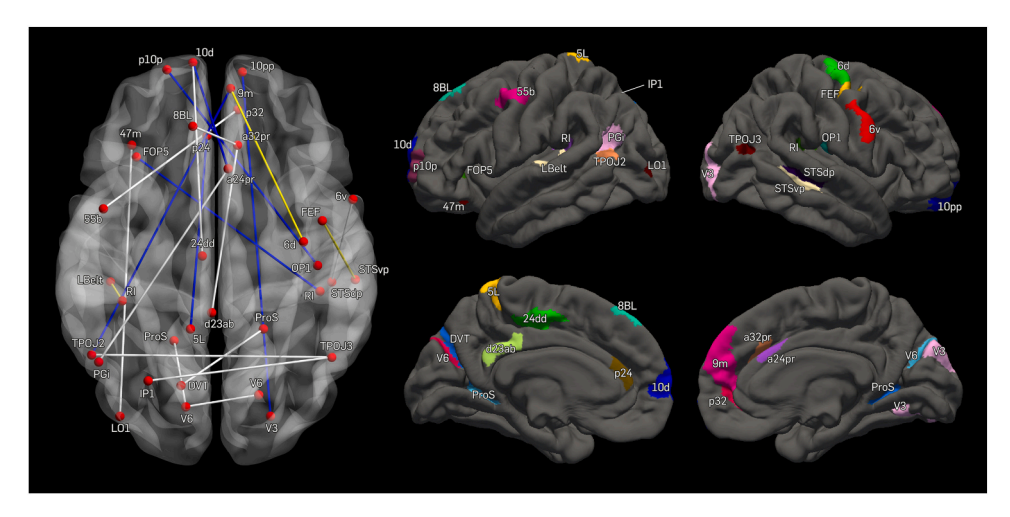


Fig. 3. Learning-related changes in functional connectivity. On the left side, functional connections are shown as yellow, white, and blue lines connecting pairs of brain areas, which are depicted as red nodes on a semi-transparent brain. All connections had to replicate across three analyses. First, functional connectivity changes in response to fear acquisition training (corrected for multiple comparisons). Second, partial correlations between functional connectivity changes and conditioned fear responses derived from skin conductance (uncorrected). Third, group differences in functional connectivity changes (uncorrected). Yellow connections survived a cross-validation procedure for the second and third analyses that a required results to replicate across 100 % of iterations. Yellow and white connections survived the cross-validation procedure after relaxing the replication threshold to 90 %. Yellow, white, and blue connections constituted the entire set of connections when the cross-validation procedure was omitted. On the right side, all brain areas involved in the functional connections shown on the left are depicted on lateral and medial views of cortical surfaces. Naming of brain areas is based on the Human Connectome Project's multi-modal parcellation.

selection derived from the results of the second analysis was around chance level (173–386 features, 45.44–52.11 %). All results are listed in Supplementary Table 8.

In the experimental group, the majority of overlapping connections (19/21, 90.48 %), showed an increase in RSFC when comparing the measurements obtained before and after fear acquisition training. Only 2 connections showed a decrease in RSFC. These were R\_TPOJ3 - L\_IP1 (temporo-parieto-occipital junction - intraparietal sulcus) and R\_V3 -R\_10pp (visual area 3 - frontal pole). Changes in RSFC ranged from -0.0575 to 0.0960 with the connection R\_V6 - L\_V6 (visual area 6 visual area 6) exhibiting the largest RSFC increase. The partial correlations between RSFC changes and CR were positive for 19 connections (r = .2027 to. 3201) and negative for the remaining 2 connections (r = .2027 to. 3201).2244 and -.3095). The strongest positive correlation was shown by connection L V6 - L ProS (visual area 6 - area prostriata) and the strongest negative correlation by connection R TPOJ3 - L IP1 (temporoparieto-occipital junction - intraparietal sulcus). In the control group, pre- vs. post-acquisition RSFC changes showed more decreases (13/21, 61.90 %) than increases (8/21, 38.10 %) and were in the range between -0.0374 and 0.2045. Consequentially, group differences in RSFC changes primarily resulted from RSFC increasing in the experimental group and decreasing in the control group. This was the case for 13 out of 21 connections. Interestingly, all but one of the 6 connections that exhibited RSFC increases in both groups showed higher increases in the control compared to the experimental group. The group differences in RSFC change ranged from 0.0593 for the connection Lp24 - L5L (anterior cingulate cortex - superior parietal lobule) to 0.1085 for the connection R\_V6 - L\_V6 (visual area 6 - visual area 6).

#### 4. Discussion

The primary goal of this study was to investigate fear learning-associated RSFC changes in participants free of psychiatric/neurological disorders. Unlike previous studies [16,17,34,76], our approach critically differed in two ways. First, we examined all functional connections across the entire brain, avoiding preselection of fear and safety network regions. Second, we included a control group to isolate fear-specific effects. These methodological distinctions yielded novel insights discussed below. The ROI nomenclature follows the Human

Connectome Project's multimodal parcellation [27], with detailed descriptions provided in the supplementary materials to the original publication.

Our first analysis examined RSFC changes in the experimental group. Most functional connections showed positive shifts (99 % of significant results; 75 % overall), with positive correlations increasing and negative correlations decreasing or even reversing. Physiologically, this may suggest strengthened excitatory and weakened inhibitory connections. The same pattern, though less pronounced (63 % of connections), occurred in the control group. Both groups received identical instructions, i.e. to attend to images potentially paired with shock, creating an unknown/threatening situation that likely induced alertness and attention in all participants. This state was further reinforced in the experimental group by actual shocks. Research in rodents has shown that the strength of excitatory connections is significantly reduced under anesthesia compared to a wakeful state [89]. In humans, the balance between excitation and inhibition has been shown to shift towards inhibition when entering a state of low vigilance or drowsiness, e.g. after a large meal [92]. These findings are well in line with the results from our first analysis, suggesting that a state of alertness and attention might cause a shift towards excitation.

Functional connections exhibiting statistically significant RSFC changes in our first analysis were subjected to our second analysis. Here, we computed partial correlations between respective RSFC changes and CR values while using pre-acquisition RSFC measures as a control variable. None of these partial correlations survived correction for multiple comparisons. However, the 386 correlations reaching a level of  $\alpha = 0.05$ (uncorrected) yielded an interesting result, in that the vast majority of correlations turned out to be positive (about 96 % of correlations). As mentioned above, nearly all significant RSFC changes in the experimental group represented positive shifts. This indicates stronger connectivity changes were associated with higher CRs. Since CRs quantify threat-safety discrimination (CS+ minus CS- SCRs), high CR values reflect distinct physiological reactions to threat versus safety signals. Taken together, this pattern suggests participants entered an alert state during pre-training instructions, which was amplified by actual shocks in the experimental group and neurally expressed as strengthened excitatory and weakened inhibitory connections. Greater shifts led to clearer SCR differentiation, indicating enhanced fear learning with

Behavioural Brain Research 495 (2025) 115764

Table 1
Functional connections replicating across all three analyses. The table lists all functional connections that exhibited statistically significant results in the first analysis (comparison of resting-state functional connectivity measured before and after fear acquisition in the experimental group,  $\alpha = .05$  corrected), the second analysis (partial correlations between post-pre differences in resting-state functional connectivity and conditioned fear responses in the experimental group,  $\alpha = .05$  not corrected), and the third analysis (comparison of post-pre differences in resting-state functional connectivity between the experimental and control group,  $\alpha = .05$  not corrected). Results of respective analyses are separated by vertical lines. Connections highlighted in bold survived a cross-validation procedure for the second and third analyses that a required results to replicate across 90 % of iterations. Connections highlighted with an asterisk survived this procedure even after increasing the replication threshold to 100 %. Naming of brain areas is based on the Human Connectome Project's multimodal parcellation. RSFC<sub>exp,pre</sub> = mean resting-state functional connectivity between two brain areas measured before fear acquisition in the experimental group; RSFC<sub>exp,post</sub> = mean resting-state functional connectivity between two brain areas measured after fear acquisition in the experimental group; RSFC<sub>exp,post</sub> = p-values from first analysis;  $\alpha$ <sub>1</sub> =  $\alpha$ -values from first analysis (Benjamini-Hochberg corrected); RSFC<sub>con,diff</sub> = difference between resting-state functional connectivity measured before and after fear acquisition in the control group; p<sub>3</sub> = p-values from third analysis (Benjamini-Hochberg corrected).

ROI A	ROI B	$RSFC_{exp\_pre}$	RSFC <sub>exp_post</sub>	RSFC <sub>exp_diff</sub>	$p_1$	$lpha_1$	r	$p_2$	$lpha_2$	$RSFC_{exp\_diff}$	$RSFC_{con\_diff}$	RSFC <sub>exp_diff</sub> - RSFC <sub>con_diff</sub>	<i>p</i> <sub>3</sub>	$lpha_3$
R_a32pr	L_d23ab	0.061715	0.109635	0.047920	0.002131	0.002159	0.246451	0.014956	0.002736	0.047920	-0.032352	0.080272	0.009969	0.001279
L_RI*	L_LBelt*	0.419894	0.463698	0.043804	0.001910	0.002043	0.236598	0.019636	0.003205	0.043804	0.117407	0.073603	0.013790	0.001635
R_a32pr	L_8BL	0.031026	0.094920	0.063895	0.001352	0.001716	0.248415	0.015769	0.002800	0.063895	-0.032895	0.096790	0.013846	0.001667
R_9m*	R_6d*	0.027784	0.094487	0.066703	0.000126	0.000509	0.221096	0.031305	0.004387	0.066703	-0.021037	0.087740	0.014647	0.001797
R_OP1	L_p10p	0.023760	0.069069	0.045309	0.000587	0.001104	0.202686	0.046474	0.005860	0.045309	-0.020005	0.065314	0.017172	0.002023
R_STSdp	R_6v	0.108672	0.162453	0.053781	0.001425	0.001772	0.234826	0.020599	0.003286	0.053781	-0.027332	0.081113	0.020615	0.002331
L_V6	L_ProS	0.332561	0.408701	0.076140	0.000588	0.001106	0.320137	0.001390	0.000421	0.076140	0.183497	0.107357	0.021108	0.002396
R_V6	L_V6	0.611140	0.707169	0.096029	0.000026	0.000232	0.231244	0.022670	0.003512	0.096029	0.204535	0.108505	0.021579	0.002509
R_TPOJ3	L_IP1	0.109015	0.050647	-0.058368	0.001330	0.001706	-0.224412	0.027118	0.003998	-0.058368	0.028032	0.086400	0.022999	0.002606
R_STSvp*	R_FEF*	0.089729	0.147768	0.058039	0.000424	0.000935	0.248543	0.014097	0.002574	0.058039	-0.020449	0.078488	0.023196	0.002622
R_p32	L_55b	-0.025352	0.033509	0.058861	0.001642	0.001893	0.239995	0.017897	0.003059	0.058861	-0.033715	0.092576	0.024014	0.002703
L_24dd	L_10d	0.050373	0.094032	0.043659	0.002164	0.002177	0.227366	0.025112	0.003739	0.043659	-0.021455	0.065114	0.026467	0.002865
R_TPOJ3	L_TPOJ2	0.347489	0.410436	0.062947	0.000189	0.000615	0.263974	0.008984	0.001716	0.062947	0.142458	0.079511	0.027232	0.002962
L_LO1	L_47m	-0.013922	0.034143	0.048065	0.001666	0.001908	-0.309533	0.002034	0.000518	0.048065	-0.017540	0.065605	0.035733	0.003529
R_ProS	L_DVT	0.292456	0.365495	0.073039	0.000065	0.000356	0.238497	0.018646	0.003124	0.073039	0.156080	0.083040	0.039139	0.003852
R_a24pr	L_10d	-0.029134	0.038158	0.067292	0.000185	0.000610	0.204261	0.044764	0.005665	0.067292	-0.003247	0.070539	0.041289	0.004030
L_p24	L_5L	0.021329	0.075187	0.053858	0.000130	0.000516	0.281469	0.005992	0.001230	0.053858	-0.005419	0.059277	0.042105	0.004095
R_V3	R_10pp	0.017973	-0.039544	-0.057517	0.000544	0.001067	0.254226	0.011977	0.002137	-0.057517	0.010214	0.067730	0.044275	0.004192
R_9m	L_TPOJ2	0.051930	0.119829	0.067900	0.000039	0.000277	0.206824	0.042092	0.005439	0.067900	0.001611	0.066288	0.046730	0.004370
R RI	L FOP5	0.162861	0.215083	0.052223	0.000852	0.001348	0.224342	0.027167	0.004030	0.052223	-0.012456	0.064679	0.047774	0.004451

robust associations between CS presentations and threat/safety. This enhancement likely stems from two factors. First, moderate acute stress during learning facilitates memory formation, especially for arousing information [36,81]. In our study, this effect might have been optimized by participant-controlled shock intensity that avoided detrimental exhaustion [44]. Second, focused attention heightens pain unpleasantness [61]. It is conceivable that participants who were more alert perceived the electrical stimulation as more unpleasant and formed stronger associations between the aversive stimuli and the cues preceding them.

The third analysis compared RSFC changes between experimental and control groups, using connections with significant changes from the first analysis. Among the 285 connections that reached a level of  $\alpha=0.05$  (uncorrected), we found that group differences in RSFC change were predominantly constituted by positive RSFC shifts in the experimental and negative RSFC shifts in the control group (about 80 % of results). Minority patterns (17 %) showed positive shifts in both groups, albeit weaker in controls. However, interpreting this as a true inverted pattern requires caution. In contrast to the experimental group, only two control group connections (R\_LBelt - L\_3a and R\_LBelt - R\_6a) survived a correction for multiple comparisons. Thus, most control group RSFC changes likely represent noise rather than meaningful effects.

Our third analysis underscores the necessity of control groups when investigating neural effects of interventions like fear acquisition training. While the within-group analysis revealed over 3000 significant RSFC changes in the experimental group, the between-group comparison showed that merely 285 of these changes were significantly higher in the experimental group, not even considering correction for multiple comparisons. Thus, 92 % of observed changes likely reflect general aspects of the paradigm rather than fear learning itself. Controlled designs are therefore essential for identifying genuine neural correlates of fear memory formation. Notably, most prior fear learning studies lack such between-group designs, with few exceptions [16,17].

Results from the second and third analyses require cautious interpretation due to non-significance after correction for multiple comparisons. In order to maximize validity, we identified overlapping results between these analyses. This revealed 21 functional connections satisfying all three criteria: Significant RSFC changes in the experimental group that also correlated with CR values and differed from control group changes. These 21 connections were constituted by a total of 35 individual ROIs because seven ROIs (L\_10d, L\_TPOJ2, L\_V6, R\_9m, R TPOJ3, R a24pr, R a32pr) were involved in two connections instead of one. Given that empirical evidence on the exact connections from our final results is scarce, the following paragraphs will discuss individual ROIs and their functional relevance for fear learning. However, it should be noted that RSFC represents intrinsic spontaneous fluctuations in the BOLD signal. While these can show spatial overlap with extrinsic taskevoked activation and deactivation patterns, they essentially reflect different brain processes [54]. Therefore, our results should be interpreted with this caveat in mind.

There was a considerable number of ROIs which partially overlapped (at least 30 % of their volume) with regions from the fear or safety networks proposed by Fullana et al. [23]. The fear network is expected to increase its activity when individuals are processing cues indicating potential threats (CS+), while the same applies to the safety network in the face of potential safety signals (CS-). A complete list of all ROIs from the Human Connectome Project's multi-modal parcellation and their overlap with the fear and safety networks is given in Supplementary Table 9.

We identified seven ROIs showing substantial overlap with the fear network: L\_p24, R\_a24pr, and R\_a32pr located along the bilateral anterior cingulate cortex; L\_24dd adjacent to these cingulate regions; R\_RI in the right retroinsular cortex; R\_FEF and L\_55b in the frontal eye fields; and L\_FOP5 in the left frontal operculum. The involvement of cingular ROIs is significant given their role in an autonomic-interoceptive network with the anterior insular cortex [55,77]. Within this network,

the anterior insula integrates cognitive, affective, and physical states while the dorsal anterior cingulate initiates autonomic and behavioral responses [56]. This integration is complemented by multimodal sensory processing (pain, temperature, visceral, vestibular inputs) in the retroinsular cortex [7], making it relevant for fear processing. Although bilateral retroinsular ROIs (R\_RI and L\_RI) appeared in our results, only R RI met the 30 % overlap criterion for the fear network. The frontal eve fields (R FEF and L 55b) are crucial for controlling saccadic eve movements and allocating spatial attention [53]. Their involvement aligns with our paradigm requiring focused attention on a specific visual element, namely the desk lamp in the office scene. The inclusion of L\_FOP5 is particularly notable when considered alongside premotor regions in our results (R 6d, R 6v, L 5L), which are associated with movement preparation [51,70,75]. It has been demonstrated that the frontal operculum and premotor cortex show increased activation during fear acquisition training, especially in anticipation of US delivery [26]. Most likely, this is due to the frontal operculum timing the onset of US delivery and the premotor cortex preparing an adequate motor response. Given our US (electrical stimulation to right index/middle fingers), left-hemisphere L 5L may inhibit involuntary right-hand movements anticipating stimulation. R 6d and R 6v likely serve similar functions despite their ipsilateral location to the stimulated hand. R\_OP1, while not meeting the 30 % overlap criterion for the fear network, constitutes the parietal operculum similar to L\_FOP5. This region processes somatosensory information [52] and serves as an integrative hub due to its connectivity with anterior parietal cortex, thalamus, and contralateral hemisphere [15], supporting higher-order somatosensory processing including perceptual learning [69].

Regarding the safety network, we identified four ROIs showing substantial overlap: L\_d23ab in the left posterior cingulate cortex, L\_8BL in left frontal cortex (Brodmann area 8), and left parietal areas L\_IP1 and L\_PGi. Adjacent areas included bilateral temporoparietal junctions (L\_TPOJ2 and R\_TPOJ3) and L\_p32 near ventromedial prefrontal cortex. While the safety network partially overlaps with the default-mode network active during low cognitive effort [71], its activation reflects active CS- processing requiring attention and evaluation [32]. L\_d23ab contributes to an extended episodic memory network, potentially encoding CS-US associations [35]. L\_8BL has been shown to activate during uncertain situations [90]. The inferior parietal lobule (including L\_IP1, L\_PGi, and adjacent L\_TPOJ2/R\_TPOJ3) shows heightened activation in contextual fear conditioning [2,6], integrating multisensory information and modulating threat attention [4,48].

In addition to brain regions from the fear and safety networks, our final analysis also revealed visual ROIs. Among these were lefthemisphere L\_ProS, L\_DVT, L\_LO1, L\_V6 and right-hemisphere R\_ProS, R\_V3, R\_V6. Prostriata (L\_ProS and R\_ProS) and dorsal transitional area (L\_DVT) mediate transitions between early visual areas and more anterior regions like posterior cingulate, providing a ventromedial visual stream to the hippocampus for scene representation [72]. Their involvement aligns with our choice of CS, namely a picture of an office environment. The lateral occipital cortex, comprising L\_LO1, is primarily associated with object and face recognition [29,62], while visual areas 3 and 6 (R\_V3, L\_V6, R\_V6) play a crucial role in the processing of motion [24,68]. To our knowledge, visual areas 3 and 6 have not been discussed in previous fMRI research on fear acquisition or fear consolidation. However, an involvement of primary visual cortex (V1) has been demonstrated in both primates [46] and humans [3,39,73,78,84]. The majority of these studies employed visual grating stimuli as CS and were able to show distinct CS+/CS- responses in V1, which processes grating orientation. Similarly, paradigms using faces as CS enhance fear network connectivity with fusiform areas [34]. Thus, visual areas processing specific CS types appear to play a critical role in fear memory acquisition and consolidation.

Beyond visual regions, we also identified frontal ROIs outside of the fear and safety networks: Brodmann area 10 subsections ( $L_10d$ ,  $L_p10p$ ,  $R_10pp$ ) and dorsomedial prefrontal  $R_9m$  (BA9). BA10 processes pain,

pain anticipation, and pain memory [65]. In the present study, participants were instructed to set the intensity of electrical stimulation to a highly aversive but not painful level. However, the circumstance that such sensations fall on a continuum and do not represent discrete categories may explain the involvement of BA10 in fear learning. R\_9m, typically linked to social cognition [47], also processes reward anticipation [37]. Its involvement may reflect reward processing when shocks were omitted during CS— and non-reinforced CS+ trials, contributing to CS value assessment.

The final step of our analysis also yielded a small number of ROIs that are hard to associate with fear learning, namely L\_LBelt, R\_STSdp, R\_STSvp, and L\_47m. These areas are involved in a broad range of tasks including auditory processing [91], motion processing [33], social cognition [27], and language [14,66]. None of these functions were required for our experiment, making it difficult to interpret the involvement of respective ROIs.

The absence of amygdala involvement in our final results was unexpected, given its well-documented role in fear acquisition [5,38,41]. However, recent meta-analyses question amygdala centrality in human fear processing [22,23,88], particularly for pain-related paradigms [9]. Methodological differences between animal and human studies warrant consideration. Animal models use intense unconditioned stimuli (e.g., foot shocks) eliciting defensive behaviors (freezing/escape) with robust amygdala activation [42], whereas human studies employ milder stimuli (e.g., tolerable shocks) rarely evoking avoidance responses. This suggests amygdala engagement may be stronger when threats directly trigger defensive actions. Methodological challenges like precise amygdala delineation in fMRI may also contribute to inconsistent findings [22,31].

As mentioned in section "2.1. Participants", the vast majority of participants recruited for this study had to be of European descent due to genetic analyses carried out for a different study utilizing the same data set. This circumstance contributed to a final sample that was rather homogenous in view of race and ethnicity. On average, participants reported that three out of their four grandparents were born in Germany. This ratio did not differ between the experimental and control group but it has to be acknowledged that this kind of sample homogeneity can impact the generalizability of findings across races. For example, Kredlow et al. [40] found that African-American participants are more likely to show very low or unmeasurable SCRs compared to non-African American participants and are therefore more often excluded from respective studies. Although none of our participants was of African-American descent, our findings should still be interpreted with care given the study sample's general lack of racial and ethnical diversity.

In conclusion, our findings suggest that fear learning is associated with changes in the strength of numerous functional resting-state connections. However, it is quite likely that many of these changes cannot be attributed to fear learning itself given that they can be observed for the experimental and control group alike. This highlights the importance of employing a proper control group whenever investigating the effects of fear acquisition or any other kind of intervention. Due to our explorative whole-brain approach and the high number of examined functional connections, many results failed to reach statistical significance. We chose to compensate for that by considering uncorrected results but only when they replicated across all analyses. Furthermore, we followed a cross-validation approach with stability selection to increase the reliability of results and reduce the risk of false positives. There are several other strategies that can be employed to address the complexity of large-scale connectivity analyses. For example, summarizing functional connectivity at the network level, such as averaging connectivity within or between established brain networks (e.g., default mode or salience networks), can reduce dimensionality and enhance interpretability. Additionally, graph theory and network analysis can characterize topological properties like local clustering or global efficiency, offering a complementary perspective on brain organization [82].

However, this approach requires predefined network models and bears the risk of oversimplifying or even overlooking local dynamics. Methods such as connectome-based predictive modeling (CPM), as described by Shen et al. [79], present a data-driven approach to predict individual behavioral outcomes, such as fear responses, from connectivity patterns. CPM's use of linear operations and feature selection makes it particularly suitable for handling large connectivity datasets efficiently. However, it may fail to analyze more complex relationships. The approach followed in our study led to a selection of functional connections mainly constituted by known brain regions from the fear and safety networks but also visual, frontal, premotor, and somatosensory regions. It is conceivable that this was the result of the employed fear acquisition paradigm targeting specific modalities, namely visual perception of presented CS+ and CS- images as well as somatosensory perception of electrical stimulation administered to the fingertips. The involvement of premotor regions could be explained by participants preparing to counteract involuntary body movements caused by electrical stimulation. Taken together, these findings can be viewed as a starting point for future research investigating the possibility of updating the traditional fear and safety networks based on modality dependencies. A highly specific elucidation of the neural underpinnings of fear learning is of paramount importance, not only for advancing our fundamental understanding of brain function, but also for its potential to inform clinical applications. As we continue to delineate the neural circuits and mechanisms governing fear learning, we are better positioned to translate empirical findings into practical interventions. Such interventions may include personalized brain stimulation techniques utilized to effectively treat anxiety disorders and related psychopathologies.

#### CRediT authorship contribution statement

Erhan Genç: Writing – review & editing, Supervision, Project administration, Methodology, Conceptualization. Nikolai Axmacher: Writing – review & editing, Supervision, Project administration, Conceptualization. Helene Selpien: Writing – review & editing, Investigation, Data curation. Christian J. Merz: Writing – review & editing, Methodology. Sebastian Ocklenburg: Writing – review & editing. Patrick Friedrich: Writing – review & editing, Investigation, Data curation. Dorothea Metzen: Writing – review & editing, Investigation, Data curation. Christoph Fraenz: Writing – review & editing, Writing – original draft, Visualization, Investigation, Formal analysis, Data curation.

## Declaration of Generative AI and AI-assisted technologies in the writing process

During the preparation of this work the authors used Elicit (Elicit Research; Covina, CA, USA) for literature search as well as Claude 3.5 Sonnet (Anthropic; San Francisco, CA, USA) and DeepSeek R1 (DeepSeek; Hangzhou, China) in order to improve language and readability. After using these tools, the authors reviewed and edited the content as needed and take full responsibility for the content of the publication.

#### Acknowledgements

This work is part of the Collaborative Research Center SFB 1280 on extinction learning (projects A02, A03, A09, and F02). It was supported by the Deutsche Forschungsgemeinschaft (DFG; project number 31680338). The authors would like to thank PHILIPS Germany (Burkhard Madler) for scientific support with the MRI measurements, Tobias Otto for general technical support, and Furkan Duman for advising us with implementing the machine learning pipeline. The authors would also like to express their gratitude to all research assistants for their support with data acquisition.

#### Appendix A. Supporting information

Supplementary data associated with this article can be found in the online version at doi:10.1016/j.bbr.2025.115764.

#### Data availability

Data will be made available on request.

#### References

- N.B. Albert, E.M. Robertson, R.C. Miall, The resting human brain and motor learning, Curr. Biol. 19 (12) (2009) 1023–1027, https://doi.org/10.1016/j. cub.200.04.028
- [2] R.P. Alvarez, A. Biggs, G. Chen, D.S. Pine, C. Grillon, Contextual fear conditioning in humans: cortical-hippocampal and amygdala contributions, J. Neurosci. 28 (24) (2008) 6211–6219, https://doi.org/10.1523/jneurosci.1246-08.2008.
- [3] M.I. Antov, E. Plog, P. Bierwirth, A. Keil, U. Stockhorst, Visuocortical tuning to a threat-related feature persists after extinction and consolidation of conditioned fear, Sci. Rep. 10 (1) (2020) 3926, https://doi.org/10.1038/s41598-020-60597-z.
- [4] J.L. Armony, R.J. Dolan, Modulation of auditory neural responses by a visual context in human fear conditioning, Neuroreport 12 (15) (2001) 3407–3411, https://doi.org/10.1097/00001756-200110290-00051.
- [5] A. Asok, A. Draper, A.F. Hoffman, J. Schulkin, C.R. Lupica, J.B. Rosen, Optogenetic silencing of a corticotropin-releasing factor pathway from the central amygdala to the bed nucleus of the stria terminalis disrupts sustained fear, Mol. Psychiatry 23 (4) (2018) 914–922, https://doi.org/10.1038/mp.2017.79.
- [6] C. Baeuchl, P. Meyer, M. Hoppstadter, C. Diener, H. Flor, Contextual fear conditioning in humans using feature-identical contexts, Neurobiol. Learn. Mem. 121 (2015) 1–11, https://doi.org/10.1016/j.nlm.2015.03.001.
- [7] E.E. Benarroch, Insular cortex: functional complexity and clinical correlations, Neurology 93 (21) (2019) 932–938, https://doi.org/10.1212/ https://doi.org/10.000000000525
- [8] Y. Benjamini, Y. Hochberg, Controlling the false discovery rate a practical and powerful approach to multiple testing, J. R. Stat. Soc. Ser. B (Stat. Methodol.) 57 (1) (1995) 289–300.
- [9] E.E. Biggs, I. Timmers, A. Meulders, J.W.S. Vlaeyen, R. Goebel, A.L. Kaas, The neural correlates of pain-related fear: a meta-analysis comparing fear conditioning studies using painful and non-painful stimuli, Neurosci. Biobehav. Rev. 119 (2020) 52–65, https://doi.org/10.1016/j.neubiorev.2020.09.016.
- [10] R.M. Birn, E.K. Molloy, R. Patriat, T. Parker, T.B. Meier, G.R. Kirk, V.A. Nair, M. E. Meyerand, V. Prabhakaran, The effect of scan length on the reliability of resting-state fMRI connectivity estimates, Neuroimage 83 (2013) 550–558, https://doi.org/10.1016/j.neuroimage.2013.05.099.
- [11] T.P.K. Breckel, C.M. Thiel, E.T. Bullmore, A. Zalesky, A.X. Patel, C. Giessing, Long-term effects of attentional performance on functional brain network topology, PLoS ONE 8 (9) (2013).
- [12] M.G. Craske, D. Hermans, D. Vansteenwegen, Fear and learning: from basic processes to clinical implications, American Psychological Association, 2006.
- [13] A.M. Dale, B. Fischl, M.I. Sereno, Cortical surface-based analysis. I. segmentation and surface reconstruction, Neuroimage 9 (2) (1999) 179–194.
- [14] M. Dapretto, S.Y. Bookheimer, Form and content: dissociating syntax and semantics in sentence comprehension, Neuron 24 (2) (1999) 427–432, https://doi. org/10.1016/s0896-6273(00)80855-7.
- [15] S.B. Eickhoff, S. Jbabdi, S. Caspers, A.R. Laird, P.T. Fox, K. Zilles, T.E. Behrens, Anatomical and functional connectivity of cytoarchitectonic areas within the human parietal operculum, J. Neurosci. 30 (18) (2010) 6409–6421, https://doi. org/10.1523/jneurosci.5664-09.2010.
- [16] P. Feng, T.Y. Feng, Z.C. Chen, X. Lei, Memory consolidation of fear conditioning: Bi-stable amygdala connectivity with dorsal anterior cingulate and medial prefrontal cortex, Soc. Cogn. Affect Neurosci. 9 (11) (2014) 1730–1737, https://doi.org/10.1093/scan/nst170.
- [17] T.Y. Feng, P. Feng, Z.C. Chen, Altered resting-state brain activity at functional MRI during automatic memory consolidation of fear conditioning, Brain Res. 1523 (2013) 59–67, https://doi.org/10.1016/j.brainres.2013.05.039.
- [18] B. Fischl, D.H. Salat, E. Busa, M. Albert, M. Dieterich, C. Haselgrove, A. van der Kouwe, R. Killiany, D. Kennedy, S. Klaveness, A. Montillo, N. Makris, B. Rosen, A. M. Dale, Whole brain segmentation: automated labeling of neuroanatomical structures in the human brain, Neuron 33 (3) (2002) 341–355.
- [19] B. Fischl, M.I. Sereno, A.M. Dale, Cortical surface-based analysis. Ii: inflation, flattening, and a surface-based coordinate system, Neuroimage 9 (2) (1999) 195–207.
- [20] R.A. Fisher, On the probable error of a coefficient of correlation deduced from a small sample, Metron 1 (1921) 3–32.
- [21] M.D. Fox, M.E. Raichle, Spontaneous fluctuations in brain activity observed with functional magnetic resonance imaging, Nat. Rev. Neurosci. 8 (9) (2007) 700–711.
- [22] M.A. Fullana, A. Albajes-Eizagirre, C. Soriano-Mas, B. Vervliet, N. Cardoner, O. Benet, J. Radua, B.J. Harrison, Fear extinction in the human brain: a metaanalysis of fMRI studies in healthy participants, Neurosci. Biobehav. Rev. 88 (2018) 16–25, https://doi.org/10.1016/j.neubiorev.2018.03.002.
- [23] M.A. Fullana, B.J. Harrison, C. Soriano-Mas, B. Vervliet, N. Cardoner, A. Avila-Parcet, J. Radua, Neural signatures of human fear conditioning: an updated and

- extended meta-analysis of fMRI studies, Mol. Psychiatry 21 (4) (2016) 500–508, https://doi.org/10.1038/mp.2015.88.
- [24] M. Furlan, A.T. Smith, Global motion processing in human visual cortical areas V2 and V3, J. Neurosci. 36 (27) (2016) 7314–7324, https://doi.org/10.1523/jneurosci.0025-16.2016.
- [25] E. Genc, M.L. Schoelvinck, J. Bergmann, W. Singer, A. Kohler, Functional connectivity patterns of visual cortex reflect its anatomical organization, Cereb. Cortex 26 (9) (2016) 3719–3731.
- [26] M.R. Gilmartin, N.L. Balderston, F.J. Helmstetter, Prefrontal cortical regulation of fear learning, Trends Neurosci. 37 (8) (2014) 455–464, https://doi.org/10.1016/j. tins.2014.05.004.
- [27] M.F. Glasser, T.S. Coalson, E.C. Robinson, C.D. Hacker, J. Harwell, E. Yacoub, K. Ugurbil, J. Andersson, C.F. Beckmann, M. Jenkinson, S.M. Smith, D.C. Van Essen, A multi-modal parcellation of human cerebral cortex, Nature 536 (7615) (2016) 171–178.
- [28] E.M. Gordon, A.L. Breeden, S.E. Bean, C.J. Vaidya, Working memory-related changes in functional connectivity persist beyond task disengagement, Hum. Brain Mapp. 35 (3) (2014) 1004–1017.
- [29] K. Grill-Spector, Z. Kourtzi, N. Kanwisher, The lateral occipital complex and its role in object recognition, Vis. Res. 41 (10-11) (2001) 1409–1422, https://doi.org/ 10.1016/s0042-6989(01)00073-6.
- [30] R. Guidotti, C. Del Gratta, A. Baldassarre, G.L. Romani, M. Corbetta, Visual learning induces changes in resting-state fMRI multivariate pattern of information, J. Neurosci. 35 (27) (2015) 9786–9798.
- [31] J. Haaker, S. Maren, M. Andreatta, C.J. Merz, J. Richter, S.H. Richter, S.M. Drexler, M.D. Lange, K. Jungling, F. Nees, T. Seidenbecher, M.A. Fullana, C.T. Wotjak, T. B. Lonsdorf, Making translation work: harmonizing cross-species methodologis in the behavioural neuroscience of pavlovian fear conditioning, Neurosci. Biobehav. Rev. 107 (2019) 329–345, https://doi.org/10.1016/j.neubiorev.2019.09.020.
- [32] B.J. Harrison, M.A. Fullana, E. Via, C. Soriano-Mas, B. Vervliet, I. Martinez-Zalacain, J. Pujol, C.G. Davey, T. Kircher, B. Straube, N. Cardoner, Human ventromedial prefrontal cortex and the positive affective processing of safety signals, Neuroimage 152 (2017) 12–18, https://doi.org/10.1016/j.neuroimage.2017.02.080.
- [33] G. Hein, R.T. Knight, Superior temporal sulcus-It's my area: or is it? J. Cogn. Neurosci. 20 (12) (2008) 2125–2136, https://doi.org/10.1162/jocn.2008.20148.
- [34] E.J. Hermans, J.W. Kanen, A. Tambini, G. Fernandez, L. Davachi, E.A. Phelps, Persistence of Amygdala-Hippocampal connectivity and Multi-Voxel correlation structures during awake rest after fear learning predicts Long-Term expression of fear, Cereb. Cortex 27 (5) (2017) 3028–3041, https://doi.org/10.1093/cercor/ bhw145.
- [35] D.J. Holt, G. Coombs, M.A. Zeidan, D.C. Goff, M.R. Milad, Failure of neural responses to safety cues in schizophrenia, Arch. Gen. Psychiatry 69 (9) (2012) 803, 903
- [36] M. Joels, Z. Pu, O. Wiegert, M.S. Oitzl, H.J. Krugers, Learning under stress: how does it work? Trends Cogn. Sci. 10 (4) (2006) 152–158, https://doi.org/10.1016/j. tics.2006.02.002.
- [37] T. Kahnt, J. Heinzle, S.Q. Park, J.D. Haynes, The neural code of reward anticipation in human orbitofrontal cortex, Proc. Natl. Acad. Sci. 107 (13) (2010) 6010–6015, https://doi.org/10.1073/pnas.0912838107.
- [38] D.C. Knight, C.N. Smith, D.T. Cheng, E.A. Stein, F.J. Helmstetter, Amygdala and hippocampal activity during acquisition and extinction of human fear conditioning, Cogn. Affect. Behav. Neurosci. 4 (3) (2004) 317–325, https://doi. org/10.3758/cabn.4.3.317.
- [39] D.C. Knight, C.N. Smith, E.A. Stein, F.J. Helmstetter, Functional MRI of human pavlovian fear conditioning: patterns of activation as a function of learning, Neuroreport 10 (17) (1999) 3665–3670.
- [40] M.A. Kredlow, S.L. Pineles, S.S. Inslicht, M.F. Marin, M.R. Milad, M.W. Otto, S. P. Orr, Assessment of skin conductance in African American and Non-African American participants in studies of conditioned fear, Psychophysiology 54 (11) (2017) 1741–1754, https://doi.org/10.1111/psyp.12909.
- [41] K.S. LaBar, J.C. Gatenby, J.C. Gore, J.E. LeDoux, E.A. Phelps, Human amygdala activation during conditioned fear acquisition and extinction: a mixed-trial fMRI study, Neuron 20 (5) (1998) 937–945, https://doi.org/10.1016/s0896-6273(00) 80475-4
- [42] M.R. Lamprea, F.P. Cardenas, D.M. Vianna, V.M. Castilho, S.E. Cruz-Morales, M. L. Brandao, The distribution of fos immunoreactivity in rat brain following freezing and escape responses elicited by electrical stimulation of the inferior colliculus, Brain Res. 950 (1-2) (2002) 186–194, https://doi.org/10.1016/s0006-8993(02) 03036-6.
- [43] L. Laux, P. Glanzmann, P. Schaffner, C.D. Spielberger, Das State-Trait-Angstinventar. Theoretische Grundlagen und Handanweisung, Beltz Test GmbH, 1981.
- [44] J.A. LePine, M.A. LePine, C.L. Jackson, Challenge and hindrance stress: relationships with exhaustion, motivation to learn, and learning performance, J. Appl. Psychol. 89 (5) (2004) 883–891, https://doi.org/10.1037/0021-9010.89.5.883.
- [45] C.M. Lewis, A. Baldassarre, G. Committeri, G.L. Romani, M. Corbetta, Learning sculpts the spontaneous activity of the resting human brain, Proc. Natl. Acad. Sci. 106 (41) (2009) 17558–17563, https://doi.org/10.1073/pnas.0902455106.
- [46] Z. Li, A. Yan, K. Guo, W. Li, Fear-Related signals in the primary visual cortex, Curr. Biol. 29 (23) (2019) 4078–4083, https://doi.org/10.1016/j.cub.2019.09.063.
- [47] M.D. Lieberman, M.A. Straccia, M.L. Meyer, M. Du, K.M. Tan, Social, self, (situational), and affective processes in medial prefrontal cortex (MPFC): causal, multivariate, and reverse inference evidence, Neurosci. Biobehav. Rev. 99 (2019) 311–328, https://doi.org/10.1016/j.neubiorev.2018.12.021.

- [48] D. Lloyd, I. Morrison, N. Roberts, Role for human posterior parietal cortex in visual processing of aversive objects in peripersonal space, J. Neurophysiol. 95 (1) (2006) 205–214, https://doi.org/10.1152/jn.00614.2005.
- [49] T.B. Lonsdorf, M. Klingelhöfer-Jens, M. Andreatta, T. Beckers, A. Chalkia, A. Gerlicher, V.L. Jentsch, S.M. Drexler, G. Mertens, J. Richter, Navigating the garden of forking paths for data exclusions in fear conditioning research, eLife (2019) 8.
- [50] T.B. Lonsdorf, C.J. Merz, More than just noise: Inter-individual differences in fear acquisition, extinction and return of fear in humans - biological, experiential, temperamental factors, and methodological pitfalls, Neurosci. Biobehav. Rev. 80 (2017) 703–728, https://doi.org/10.1016/j.neubiorev.2017.07.007.
- [51] T.N. Mackenzie, A.Z. Bailey, P.Y. Mi, P. Tsang, C.B. Jones, A.J. Nelson, Human area 5 modulates corticospinal output during movement preparation, Neuroreport 27 (14) (2016) 1056–1060, https://doi.org/10.1097/wnr.00000000000000555.
- [52] M.D. Maliia, C. Donos, A. Barborica, I. Popa, J. Ciurea, S. Cinatti, I. Mindruta, Functional mapping and effective connectivity of the human operculum, Cortex 109 (2018) 303–321, https://doi.org/10.1016/j.cortex.2018.08.024.
- [53] J. Martinez-Trujillo, Visual attention in the prefrontal cortex, Annu. Rev. Vis. Sci. 2 (8) (2022) 407–425, https://doi.org/10.1146/annurev-vision-100720-031711.
- [54] R. Masharipov, I. Knyazeva, A. Korotkov, D. Cherednichenko, M. Kireev, Comparison of whole-brain task-modulated functional connectivity methods for fMRI task connectomics, Commun. Biol. 7 (1) (2024) 1402, https://doi.org/ 10.1038/s42003-024-07088-3.
- [55] M. Mechias, A. Etkin, R. Kalisch, A meta-analysis of instructed fear studies: implications for conscious appraisal of threat, Neuroimage 49 (2) (2010) 1760–1768
- [56] N. Medford, H.D. Critchley, Conjoint activity of anterior insular and anterior cingulate cortex: awareness and response, Brain Struct. Funct. 214 (5-6) (2010) 535-540
- [57] R.C. Miall, E.M. Robertson, Functional imaging: is the resting brain resting? Curr. Biol. 16 (23) (2006) 998–1000, https://doi.org/10.1016/j.cub.2006.10.041.
- [58] M.R. Milad, G.J. Quirk, Fear extinction as a model for translational neuroscience: ten years of progress, Annu. Rev. Psychol. 63 (2012) 129–151, https://doi.org/ 10.1146/annurev.psych.121208.131631.
- [59] M.R. Milad, C.I. Wright, S.P. Orr, R.K. Pitman, G.J. Quirk, S.L. Rauch, Recall of fear extinction in humans activates the ventromedial prefrontal cortex and hippocampus in concert, Biol. Psychiatry 62 (5) (2007) 446–454, https://doi.org/ 10.1016/j.bjonsych.2006.10.011.
- [60] S. Mineka, K. Oehlberg, The relevance of recent developments in classical conditioning to understanding the etiology and maintenance of anxiety disorders, Acta Psychol. 127 (3) (2008) 567–580.
- [61] D. Miron, G.H. Duncan, C.M. Bushnell, Effects of attention on the intensity and unpleasantness of thermal pain, Pain 39 (3) (1989) 345–352, https://doi.org/ 10.1016/0304-3959(89)90048-1.
- [62] K. Nagy, M.W. Greenlee, G. Kovacs, The lateral occipital cortex in the face perception network: an effective connectivity study, Front. Psychol. 3 (2012), https://doi.org/10.3389/fpsyg.2012.00141.
- [63] R.C. Oldfield, The assessment and analysis of handedness: the Edinburgh inventory, Neuropsychologia 9 (1) (1971) 97–113.
- [64] W.D. Oswald, E. Roth, Der Zahlen-Verbindungs-Test (ZVT), Hogrefe, 1987.
- [65] K. Peng, S.C. Steele, L. Becerra, D. Borsook, Brodmann area 10: collating, integrating and high level processing of nociception and pain, Prog. Neurobiol. 161 (2018) 1–22
- [66] L.A. Petitto, R.J. Zatorre, K. Gauna, E.J. Nikelski, D. Dostie, A.C. Evans, Speech-like cerebral activity in profoundly deaf people processing signed languages: implications for the neural basis of human language, Proc. Natl. Acad. Sci. 97 (25) (2000) 13961–13966, https://doi.org/10.1073/pnas.97.25.13961.
- [67] E.A. Phelps, Human emotion and memory: interactions of the amygdala and hippocampal complex, Curr. Opin. Neurobiol. 14 (2) (2004) 198–202, https://doi. org/10.1016/j.comb.2004.03.015
- [68] S. Pitzalis, P. Fattori, C. Galletti, The functional role of the medial motion area V6, Front. Behav. Neurosci. 6 (2012), https://doi.org/10.3389/fnbeh.2012.00091.
- [69] B. Pleger, A.F. Foerster, P. Ragert, H.R. Dinse, P. Schwenkreis, J.P. Malin, V. Nicolas, M. Tegenthoff, Functional imaging of perceptual learning in human primary and secondary somatosensory cortex, Neuron 40 (3) (2003) 643–653, https://doi.org/10.1016/s0896-6273(03)00677-9
- [70] A. Premji, N. Rai, A. Nelson, Area 5 influences excitability within the primary motor cortex in humans, PLoS ONE 6 (5) (2011), https://doi.org/10.1371/journal. pone.0020023.
- [71] M.E. Raichle, The brain's default mode network, Annu. Rev. Neurosci. 38 (2015) 433–447.

- [72] E.T. Rolls, S. Wirth, G. Deco, C.C. Huang, J. Feng, The human posterior cingulate, retrosplenial, and medial parietal cortex effective connectome, and implications for memory and navigation, Hum. Brain Mapp. 44 (2) (2023) 629–655, https://doi. org/10.1002/hbm.26089.
- [73] A. Santos-Mayo, S. Moratti, How fear conditioning affects the visuocortical processing of context cues in humans. evidence from steady state visual evoked responses, Cortex 183 (2025) 21–37, https://doi.org/10.1016/j. cortex.2024.11.005.
- [74] L. Schlaffke, L. Schweizer, N.N. Rüther, R. Luerding, M. Tegenthoff, C. Bellebaum, T. Schmidt-Wilcke, Dynamic changes of resting state connectivity related to the acquisition of a lexico-semantic skill, Neuroimage 146 (2017) 429–437.
- [75] R.I. Schubotz, D.Y. von Cramon, Functional-anatomical concepts of human premotor cortex: evidence from fMRI and PET studies, Neuroimage 20 (2003) 120–131, https://doi.org/10.1016/j.neuroimage.2003.09.014.
- [76] D.H. Schultz, N.L. Balderston, F.J. Helmstetter, Resting-state connectivity of the amygdala is altered following pavlovian fear conditioning, Front. Hum. Neurosci. 6 (2012), https://doi.org/10.3389/fnhum.2012.00242.
- [77] C. Sehlmeyer, S. Schoning, P. Zwitserlood, B. Pfleiderer, T. Kircher, V. Arolt, C. Konrad, Human fear conditioning and extinction in neuroimaging: a systematic review, PLoS ONE 4 (6) (2009), https://doi.org/10.1371/journal.pone.0005865.
- [78] L. Shalev, R. Paz, G. Avidan, Visual aversive learning compromises sensory discrimination, J. Neurosci. 38 (11) (2018) 2766–2779.
- [79] X. Shen, E.S. Finn, D. Scheinost, M.D. Rosenberg, M.M. Chun, X. Papademetris, R. T. Constable, Using connectome-based predictive modeling to predict individual behavior from brain connectivity, Nat. Protoc. 12 (3) (2017) 506–518, https://doi.org/10.1038/nprot.2016.178.
- [80] T. Sherif, P. Rioux, M. Rousseau, N. Kassis, N. Beck, R. Adalat, S. Das, T. Glatard, A. C. Evans, CBRAIN: a web-based, distributed computing platform for collaborative neuroimaging research, Front. Neuroinformatics 8 (2014).
- [81] T. Smeets, O.T. Wolf, T. Giesbrecht, K. Sijstermans, S. Telgen, M. Joels, Stress selectively and lastingly promotes learning of context-related high arousing information, Psychoneuroendocrinology 34 (8) (2009) 1152–1161, https://doi. org/10.1016/j.psyneuen.2009.03.001.
- [82] O. Sporns, The human connectome: a complex network, Ann. N. Y Acad. Sci. 1224 (2011) 109–125, https://doi.org/10.1111/j.1749-6632.2010.05888.x.
- [83] Y. Stegmann, M.A. Schiele, D. Schumann, T.B. Lonsdorf, P. Zwanzger, M. Romanos, A. Reif, K. Domschke, J. Deckert, M. Gamer, P. Pauli, Individual differences in human fear generalization-pattern identification and implications for anxiety disorders, Transl. Psychiatry 9 (1) (2019) 307, https://doi.org/10.1038/s41398-019-0646-8.
- [84] M. Stolarova, A. Keil, S. Moratti, Modulation of the C1 visual event-related component by conditioned stimuli: evidence for sensory plasticity in early affective perception, Cereb. Cortex 16 (6) (2006) 876–887.
- [85] K. Tabbert, C.J. Merz, T. Klucken, J. Schweckendiek, D. Vaitl, O.T. Wolf, R. Stark, Influence of contingency awareness on neural, electrodermal and evaluative responses during fear conditioning, Soc. Cogn. Affect Neurosci. 6 (4) (2011) 495–506, https://doi.org/10.1093/scan/nsq070.
- [86] K. Tung, J. Uh, D. Mao, F. Xu, G. Xiao, H. Lu, Alterations in resting functional connectivity due to recent motor task, Neuroimage 78 (2013) 316–324.
- [87] J. Tzschoppe, F. Nees, T. Banaschewski, G.J. Barker, C. Buchel, P.J. Conrod, H. Garavan, A. Heinz, E. Loth, K. Mann, J.L. Martinot, M.N. Smolka, J. Gallinat, A. Strohle, M. Struve, M. Rietschel, G. Schumann, H. Flor, I. consortium, Aversive learning in adolescents: modulation by amygdala-prefrontal and amygdala-hippocampal connectivity and neuroticism, Neuropsychopharmacology 39 (4) (2014) 875–884, https://doi.org/10.1038/npp.2013.287.
- [88] R.M. Visser, J. Bathelt, H.S. Scholte, M. Kindt, Robust BOLD responses to faces but not to conditioned threat: challenging the amygdala's reputation in human fear and extinction learning, J. Neurosci. 41 (50) (2021) 10278–10292, https://doi. org/10.1523/jneurosci.0857-21.2021.
- [89] J.A. Vizuete, S. Pillay, K. Diba, K.M. Ropella, A.G. Hudetz, Monosynaptic functional connectivity in cerebral cortex during wakefulness and under graded levels of anesthesia, Front. Integr. Neurosci. 6 (2012), https://doi.org/10.3389/ fnint.2012.00090.
- [90] K.G. Volz, R.I. Schubotz, D.Y. von Cramon, Variants of uncertainty in decision-making and their neural correlates, Brain Res. Bull. 67 (5) (2005) 403–412, https://doi.org/10.1016/j.brainresbull.2005.06.011.
- [91] J.D. Warren, T.D. Griffiths, Distinct mechanisms for processing spatial sequences and pitch sequences in the human auditory brain, J. Neurosci. 23 (13) (2003) 5799–5804, https://doi.org/10.1523/jneurosci.23-13-05799.2003.
- [92] B. Yang, H. Zhang, T. Jiang, S. Yu, Natural brain state change with E/I balance shifting toward inhibition is associated with vigilance impairment, iScience 26 (10) (2023), https://doi.org/10.1016/j.isci.2023.107963.